

variation, peaking in 2006 and 2019, with its long-term pattern essentially stable as per the trend line. Annual rainfall for North India shows a trend that is slightly declining in nature. There are notable declines in certain years, like 2002 and 2015. Overall, the trend is such that the annual rainfall is gradually decreasing over the study period. Similar to North India, the rainfall in South India also follows a mild negative annual rainfall trend with huge variability. This has peak rain years like 2011 and extremely dry years like 2002. In Thailand, the annual rainfall trend is also stable with rainy and dry peaks and troughs. The trend line shows a largely steady pattern without much long-term change.

4.5.2 Monthly Rainfall Trends Over Multiple Years

Later, we examined the trend of monthly rainfall from 22 years. By grouping spatial averages by month across many years allows one to distinguish variability in the same month in different years, such as rainfall in January over different years between 1998 and 2019. This way, it explicitly captures the variation in monthly rainfall from year to year, detail that may be lost if only the annual totals are taken as relevant. To visually assess how precipitation has changed over time within a particular month, separate bar plots were created for each month. This is a good way to see precisely which year was unusually wet or dry for each month, and which can then be related to particular climatic events or anomalies such as El Niño or La Niña. As shown in the Figure 4.4, the rainfall trends from 1998 to 2019 for Central India, North India, South India, Indonesia, and Malaysia, the trend has huge variability with marked regional differences. Certain fluctuations are visible in Central India, particularly for October and September, peaking around the early 2000s and 2010 with a marked rise for September toward 2020. In April and December, relatively consistent trends can be seen, but in months like July and May, one observes declining rain in the later years. Rainfall in North India varied in intensity, peaking throughout winter months—for example, the month of January and February of the years 2005 and 2015. In June and July, conditions are much more stable, with small-scale fluctuations; for the remaining months, such as October and November, conditions are more unstable, peaking sharply during November 2020. Mixed patterns are seen in south India from a relatively stable pattern in the months of July and August to variability in January and February, peaking around 2010; a generalized decrease in April and June toward 2020. Indonesia and Malaysia have more regular trends in rainfall than India, peaking around 2010 for many months, such as September, October, and November. Indonesia is very stable in terms of rainfall variability, while Malaysia has more fluctuations in rainfall, especially in June and November, peaking for some months around 2010 and then slightly falling toward 2020. Overall, data from all regions demonstrate a high inter-annual variability. No long-term rainfall trend can be observed, suggesting that the regional climatic and environmental factors might contribute to such a pattern. Observed trends seem to intimate that changes in water resource availability and agricultural practices may have to be considered arising from variations in rainfall.

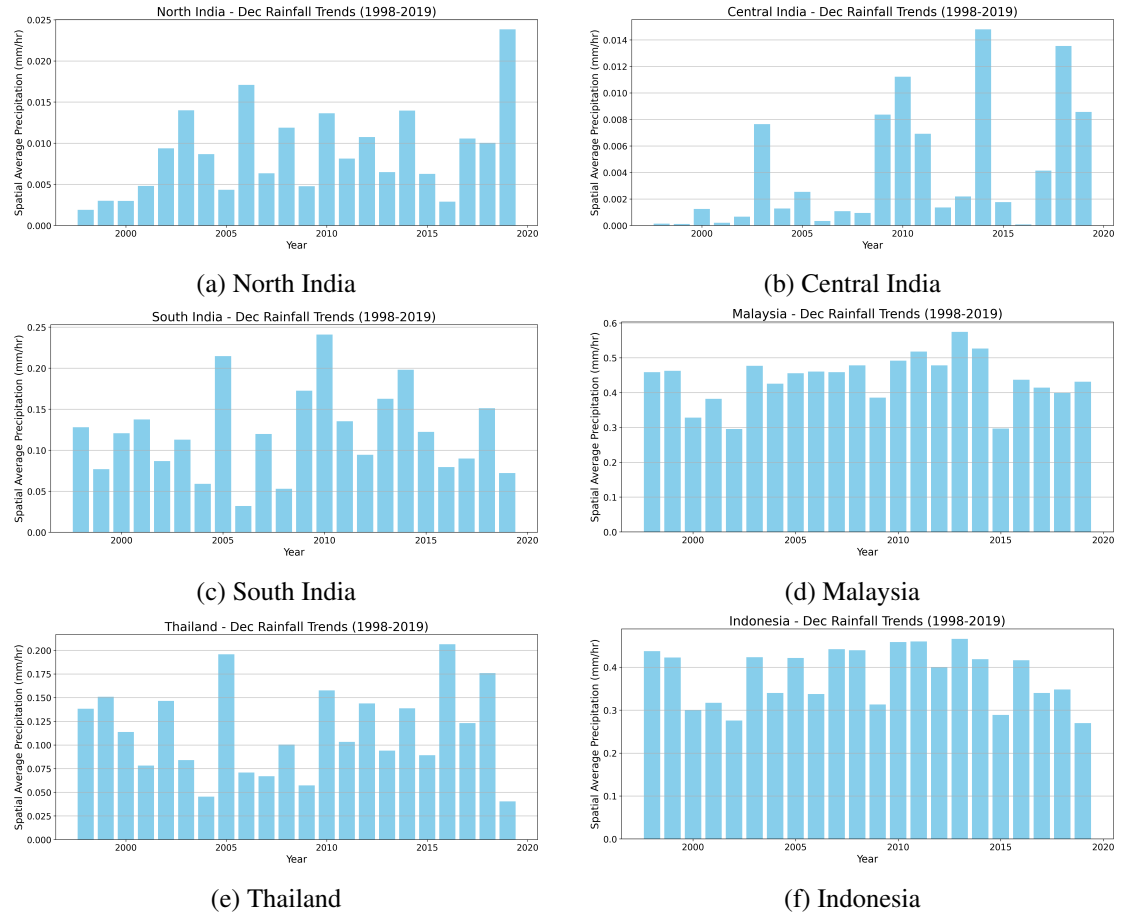


Figure 4.4: Monthly rainfall trend over multiple years (December)

4.5.3 Seasonal Cycle Analysis

The seasonal cycle analysis was performed to determine which is the average precipitation pattern of each month for the 22-year period. The usually wettest and driest months in each region can be indicated by averaging all years for each month, with the characteristic seasonal behaviour reflecting monsoon cycles, dry seasons, and other large-scale climatic influences. This work provides a base-level understanding of the average seasonal cycle for each region against which anomalies and trends can be calculated. In some regions, especially those that rely heavily on predictable seasonal rainfall-for example, due to monsoon rains for agriculture-this can be extremely important. In fact, having a more complete idea of the normal seasonal cycle helps in predicting the effects of any variation from this pattern, whether short-term anomalies or long-term shifts. As shown in the Figure 4.5, the monsoon dominates the seasonality of Central India, with rainfall peaking in July and August. Rainfall is very low, highly significantly so, between the months of January to May and October to December, and hence this is a climate that is strongly of the type dominated by the monsoon. Indonesia shows consistent rainfall seasonality than Central India, but slight peaks of rainfall in December and January. This indicates

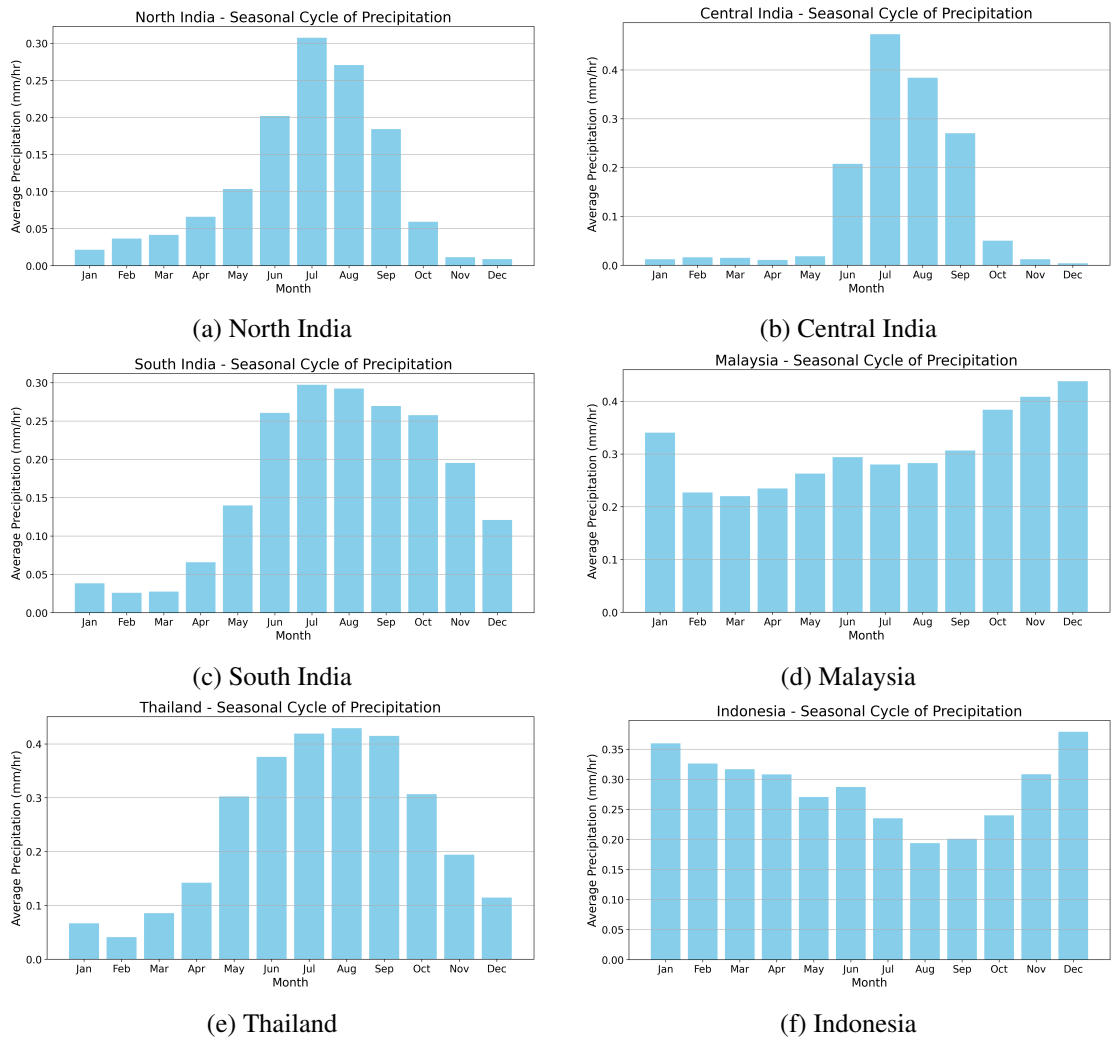


Figure 4.5: Seasonal Cycle Analysis

the equatorial regime over Indonesia, as there is no pronounced dry season over this region. Malaysia has a bimodal seasonal cycle—a maximum in rainfall during the months of November–December followed by another peak during June–July—corresponding to the northeast monsoon and southwest monsoon, respectively. The rainfall in this region is rather evenly distributed throughout the year. No month can be considered a really dry month. Like Central India, North India also has a seasonal cycle dominated by the monsoon when most of the rains fall between June and September; for the rest of the year, rainfall is scanty. For the rest of the year, the period is relatively dry, receiving scanty rainfall. South India receives its share of rainfall during the monsoon, but it still continues to get considerable rainfall during both the southwest monsoon from June to September and the northeast monsoon during the months of October–November. The seasonal cycle is relatively higher throughout the year than in North India. In Thailand, this seasonal cycle is greatly influenced by the monsoon; the bulk of the rain falls between June and October. Rest of the year is comparatively dry, with precipitation falling drastically after

November onwards.

4.6 Summary

Regional analysis brings out the widespread variation in the pattern of precipitation. Central India and North India reveal a marked monsoonal influence with heavy rainfall during the monsoon months and scanty precipitation during the rest of the year. Indonesia and Malaysia lie in the equatorial belt; thus, their rainfall is better distributed throughout the year, as befits their tropical climates. The southwest and northeast monsoons shape the climate of south India in such a way that there are two peaks in rainfall. Thailand follows a similar pattern to that of the Indian subcontinent concerning the major linkage of its rainfall to the months associated with the monsoon. This analysis, while putting together annual trends, monthly variability, and seasonal cycles, provides a broad understanding of regional precipitation patterns.

Chapter 5

Precipitation and Smoothened Precipitation Anomalies

The time series analysis on the previous chapter gave an overview of general trends and patterns over time. Variability and extremes in precipitation cannot be ascertained without analysing the deviations from such trends, more commonly referred to as anomalies. It is important to note that precipitation anomalies, as deviations from the long-term average conditions, are key to understanding extreme weather events, such as droughts and excessive rainfall these cannot be realized simply by examining raw precipitation data. These anomalies thereby could be used to deduce the intensity, frequency, and duration of the rainfall anomaly events, usually related to the larger-scale climatic indices such as ENSO and IOD. These computed anomalies have an important bearing on intra-regional climate variability, water resources, and agriculture. This chapter deals with computation of precipitation anomalies and their monthly variation, and smoothed anomaly, which tends to give better representation of the long-term trends by filtering out a lot of the short-term variability.

5.1 Precipitation Anomalies

Precipitation anomalies are calculated to determine how far the precipitation amount for a particular month or period has varied from the long-term average of that same month or period. It is done by determining, for each area of the region, the long-term monthly mean precipitation by averaging all the precipitation values of each month of the period being considered. First, the anomaly for each month and year is computed by subtracting the long term monthly mean from the observed monthly precipitation. This is expressed mathematically by:

$$\text{Anomaly} = \text{Observed Monthly Precipitation} - \text{Long-term Monthly Mean},$$

the calculation helps in the identification of peculiar conditions of weather that might include a very high or low amount of precipitation in comparison to average. It becomes important for

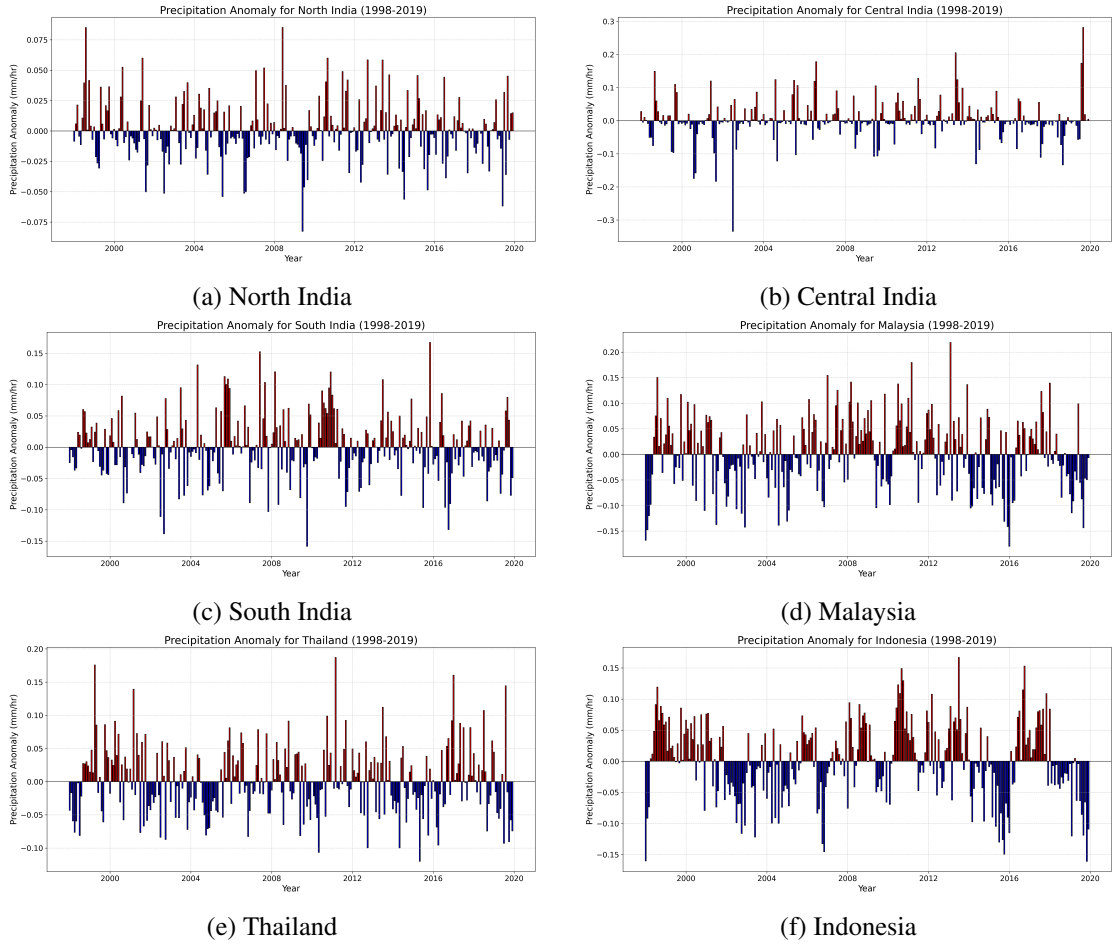


Figure 5.1: Precipitation Anomalies

understanding how regional climates deviate from expected patterns, in response to large-scale climatic events such as ENSO and IOD. As shown in the Figure 5.1, the precipitation anomalies for Central India are quite variable: large positive anomalies in 1999, 2005, and 2019 reflect years with excessive rain. These denote the excessive rainfalls of those years, while on the other hand, negative anomalies, such as in 2000 and 2009, represent periods of lessened precipitation. Frequent alternations between positive and negative anomalies clearly show that this region is highly variable. Precipitation anomalies over Indonesia show distinct periods of positive and negative anomalies. The early 2000s have marked substantial positive anomalies, especially in the year 2000 and 2001, indicative of higher-than-average rainfall; however, this gave way to a period of consistent negative anomalies from 2010 to 2019 that is reflective of a possible long-term trend toward drier conditions. The data for Malaysia shows massive positive anomalies in the early 2000s, peaking in 2002. Then it experienced a sequence of negative anomalies after 2010, concurrently with a possible trend of reduced precipitation or more frequent dry spells in the region. Rainfall anomalies over North India mirror cycles of positives and negatives. These are considerable positive anomalies, such as in the years 1998, 2005, and 2013, indicative of

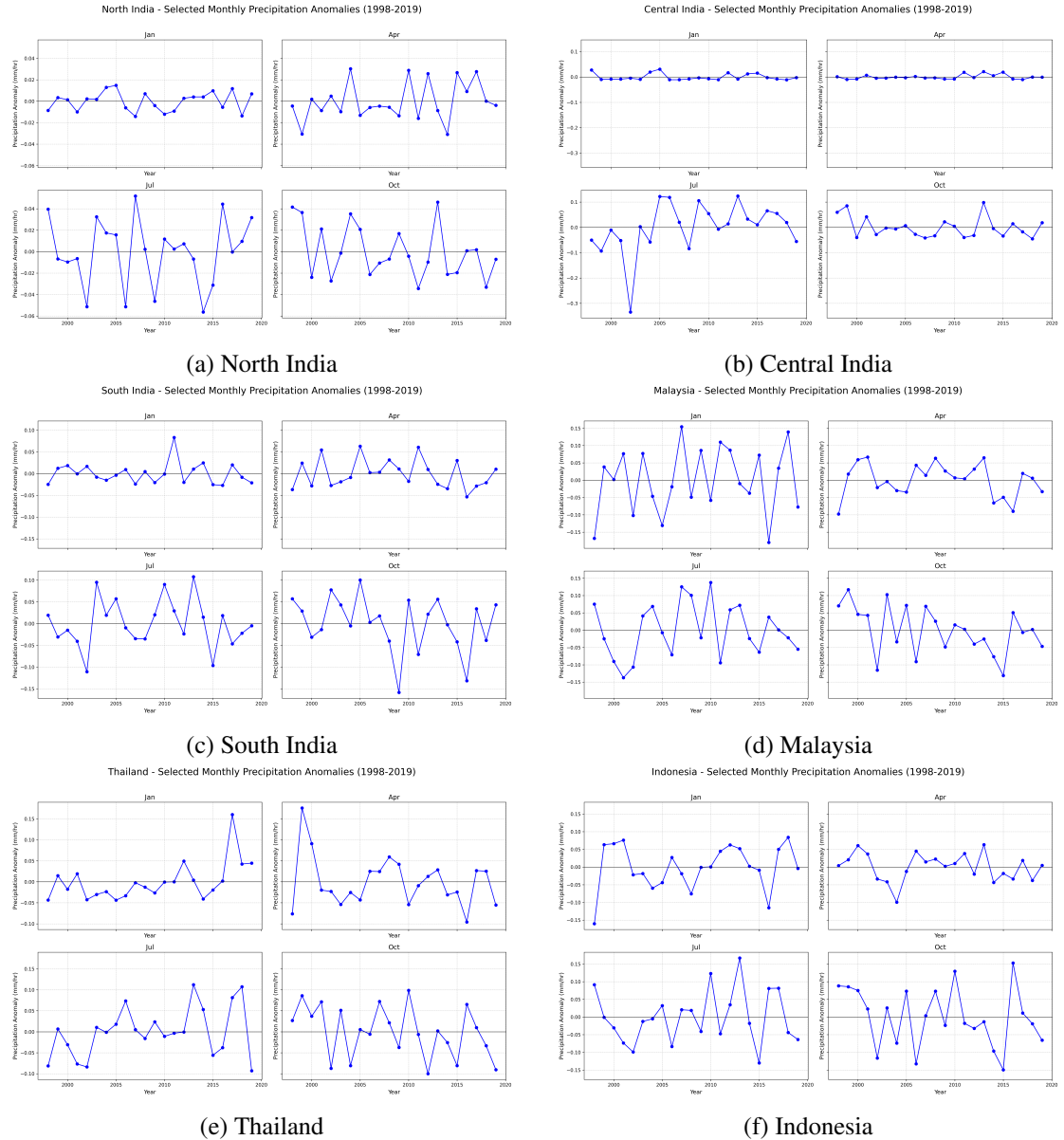


Figure 5.2: Monthly Anomalies

excessive rainfall episodes, while there are negative ones, such as in the years 2002 and 2009, which reflects drought conditions. The early 2000s show a considerable positive anomaly, with a peak in 2005. Since 2010, frequent negative anomalies have been recorded in the region, with 2015 being one of the driest years on record, pointing toward a trend of less precipitation. Precipitation anomalies over Thailand similarly reveal strong positive deviations in the years 2000 and 2006, reflecting periods of heavy rainfall. Conversely, negative anomalies dominated between 2010 and 2019, indicating drier conditions.

5.2 Monthly Anomalies

The understanding of monthly anomalies is important because it shows the seasonality and temporal properties of precipitation that could not be reflected through yearly averages only. The approach to calculating monthly anomalies follows the same approach as that used in the general precipitation anomalies, but it narrows down to the deviations that take place in each month across the years. As shown in the Figure 5.2, monthly anomalies in the Central India series are indicative of a pattern whereby some months—especially those falling between June to September—are representative of large variability. For instance, July shows distinctly large positive anomalies over many years, indicating above-average rainfall in that month. It coincides with the peak time of the monsoon period. Also, January and February are those months when the variation has remained quite stable without much anomaly. The monthly anomalies for Indonesia in the larger-scale regional context for Indonesia do show considerable variation in the wet season between months, although the major part falls between December and March. January and February present quite marked positive anomalies in the early 2000s, which should reflect wetter than normal conditions, whereas June and July are two months with relatively more stable patterns and lesser anomalies. In Malaysia, monthly anomalies show considerable variation throughout the year, particularly during the northeast monsoon months of November to January. These periods therefore tend to show frequent positive anomalies relative to periods of above-average rainfall, but during the inter-monsoon months, the patterns are relatively more stable. In North India, the monthly anomalies stand out during the months of the monsoon period, that is, between June and September. There are considerable positive anomalies during July and August in several years, indicative of heavy rains during the monsoon season. The winter months, however, reflect far more stable precipitation patterns with limited anomalies. Large monthly anomalies do indeed appear over South India during both the southwest (June to September) and northeast (October to December) monsoon seasons. October represents the generally consistent positive anomalies, reflecting the northeast monsoon contribution and an important period of rainfall in the region. Over Thailand, the largest monthly anomalies occur during the months of May through October. There are significant positive anomalies in several years during the months of July and September, thus indicating the heavy rainfall period. Precipitation during the months of the dry season is relatively stable with fewer anomalies.

5.3 Smoothened Precipitation Anomalies

Where raw anomalies are an important snapshot of deviation from normal, they can often be noisy, reflecting short-term fluctuations that may obscure the longer-term trends. In that light, we introduce the concept of smoothened precipitation anomalies that allow filtering of such noise in order to reveal the more underlying trends. Smoothing was brought about by a moving average technique, that is applying the window size of five months. In this method, the effect of short-run variation is dampened, allowing more persistent deviations to become appar-

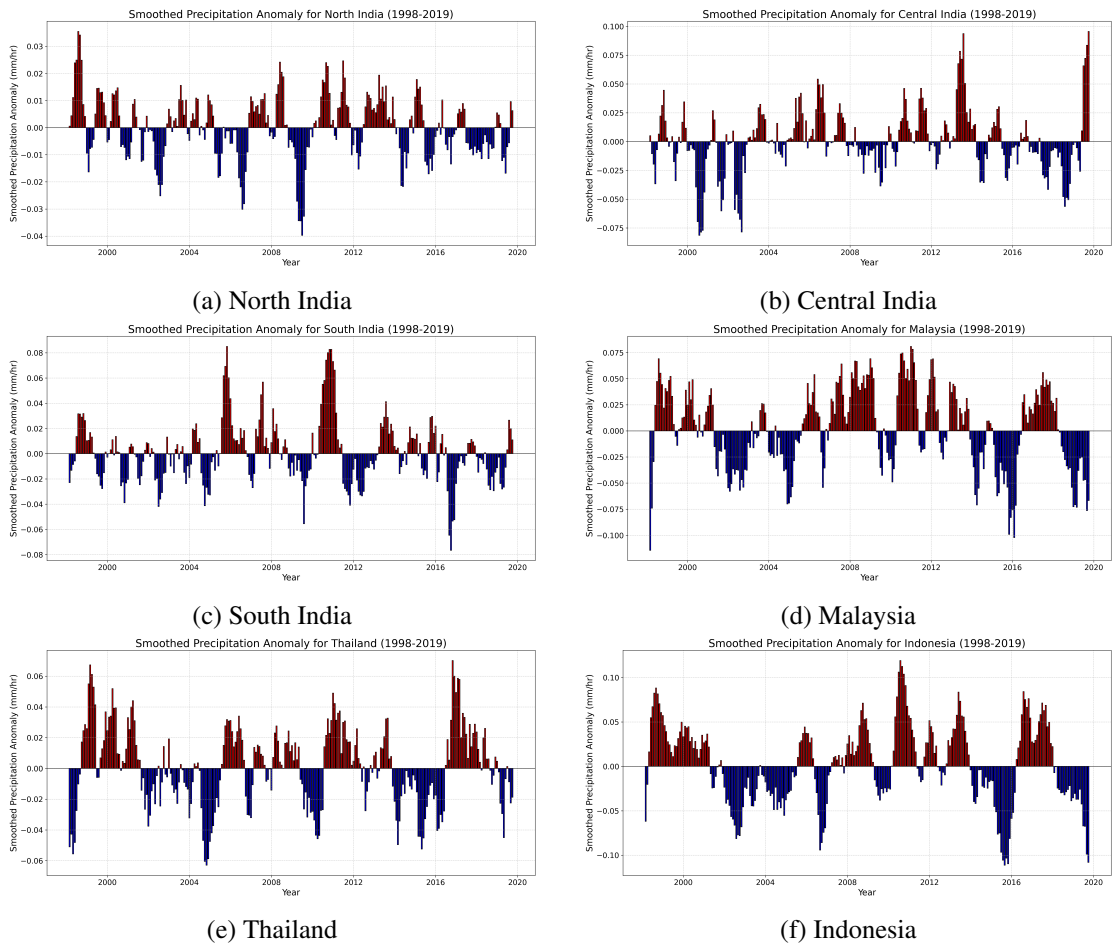


Figure 5.3: Smoothed Precipitation Anomalies

ent, reflecting longer-term changes in climate behavior rather than isolated events, refer to the Figure 5.3. This chapter develops a finer understanding of how regional climates are changing over time by analysing raw and smoothed precipitation anomalies. The analysis shows that large variability characterizes the precipitation patterns, with striking periods of excess as well as deficit in the regions under study. The smoothed anomalies bring out long-term trends that may be indicative of larger shifts in climate.

Chapter 6

Correlation with ENSO

In the previous chapters, we did an analysis of the temporal pattern of precipitation anomalies in the different regions considered, determining the most important trends and variabilities. While the previous chapters provided insights into the detailed temporal evolution of precipitation anomalies, they did not explain or show possible climatic drivers for these anomalies. It is against this background that this chapter tries to fill that gap by relating the anomalies in precipitation with one of the most influential climate phenomena: El Niño-Southern Oscillation, or ENSO. We are going to analyse how the phases of ENSO correlate with regional precipitation patterns, thus gaining insight into the degree to which ENSO explains these anomalies, with probable predictions for subsequent climatic events.

6.1 Plotting Smoothed Precipitation Anomaly along with ENSO

To evaluate the possible associations of ENSO with regional precipitation, the time series of MEI.v2 is plotted against that of the smoothed precipitation anomalies over North India, Central India, South India, Thailand, Indonesia, and Malaysia. The plots display, for each region, the smoothed precipitation anomalies in red and MEI.v2 index in blue, with a common time axis but with separated y-axes. Using a dual-axis setup provided the ability to visually discern how ENSO phases-El Niño and La Niña-further affected the precipitation patterns of these regions. There were several instances when peaks and troughs of the MEI.v2 index took their mirror opposition to the precipitation anomalies, indicating negative correlation between the two variables. The Central India plot suggests that during strong El Niño (positive MEI.v2 anomalies), the rainfall anomalies over Central India are seen to plunge, which gives below-normal rainfall. Conversely, during La Niña (negative MEI v2 anomalies), the precipitation anomalies spike, suggesting higher rainfall. As shown in the Figure 6.1, the plot gives strong emphasis on the inverse relationship for Indonesia between the MEI.v2 index and anomalies in precipitation. During El Niño, when the values of MEI.v2 are positive, Indonesia undergoes prominent rainfall reductions, indicated by the steep drops in precipitation anomalies. Similarly, Malaysia has an intensely negative relationship between ENSO phases and precipitation anomalies. The

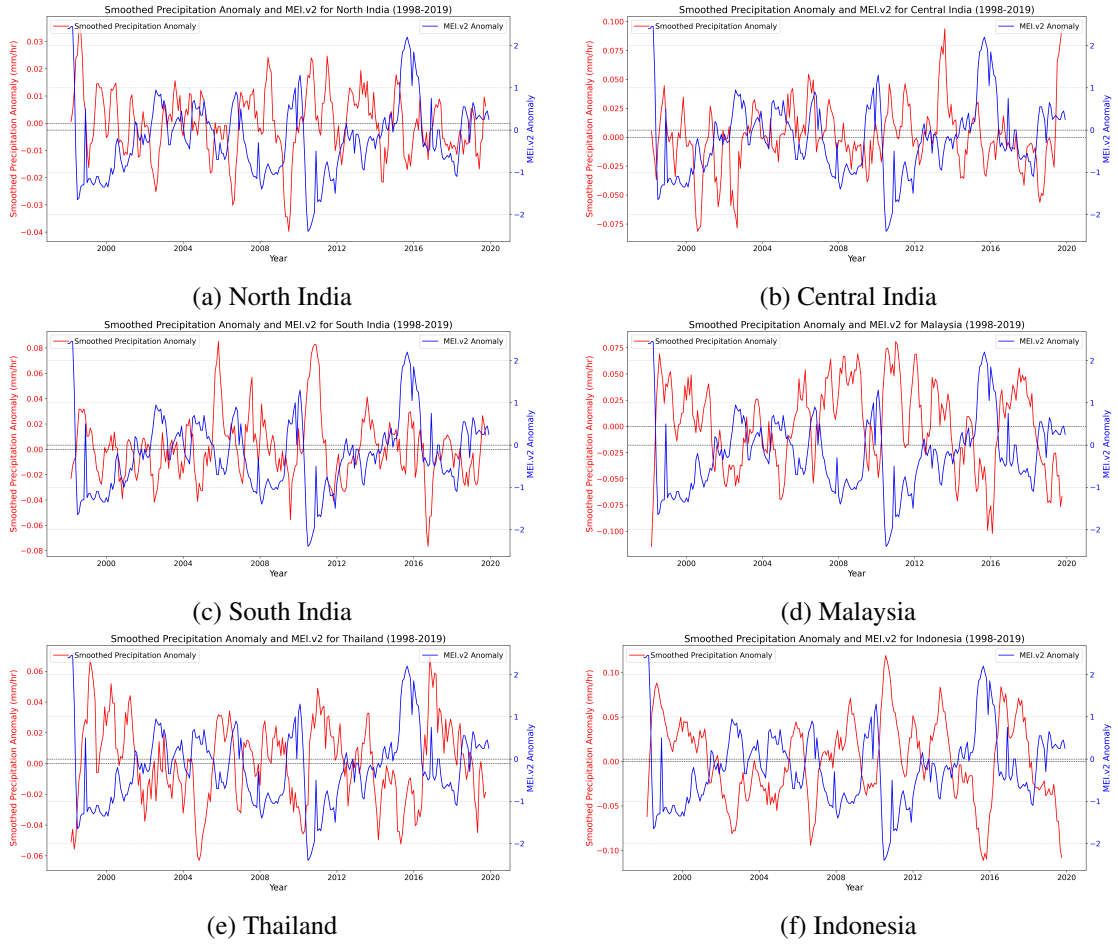


Figure 6.1: Smoothed precipitation anomaly with ENSO plot for North India, Central India, South India, Malaysia, Thailand, and Indonesia.

negative spikes in precipitation anomalies associated with El Niño events are well pronounced. The North India plot shows quite a variable relationship. Whereas the overall trend is inversely related, there are periods when precipitation anomalies don't perfectly mirror the MEI.v2 index. The plot for South India mirrors the overall trend with the other plots of regions of India—that is, it sees a fair amount of decrease in precipitation anomalies during El Niño events. The inverse relation, though, is clear and not quite as strong as that of Indonesia. The plot of Thailand, however, shows strong negative anomalies in ENSO phases with precipitation. During El Niño, the precipitation anomalies are largely negative; during La Niña, it is positive in trend.

6.2 Correlation Coefficient between ENSO and Precipitation Anomalies

In order to analyse the relationship between ENSO and regional precipitation smoothed anomalies quantitatively, we calculated the Pearson correlation coefficient between the MEI.v2 index

Region	Correlation Coefficient
North India	-0.328
Central India	-0.161
South India	-0.327
Thailand	-0.553
Indonesia	-0.745
Malaysia	-0.744

Figure 6.2: Pearson’s Correlation Coefficient for ENSO

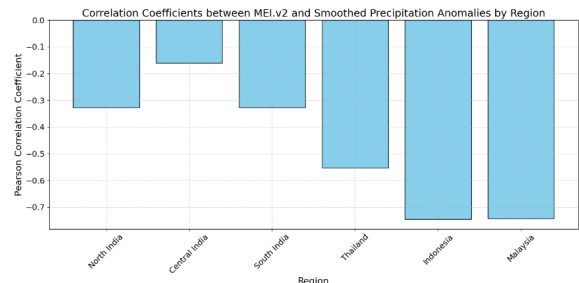


Figure 6.3: Correlation Coefficient MEI

and the smoothed precipitation anomaly of each region.

6.2.1 Pearson Correlation Coefficient

The Pearson’s correlation coefficient is one of the statistical tools used in the measurement of a linear relationship that exists between two variables, Scribbr (2022). It takes values within the range from -1 (negative linear relationship) through 0 (No linear relationship) to +1 (positive linear relationship) and is expressed by the symbol r :

$$r = \frac{\sum_{i=1}^n (X_i - \bar{X})(Y_i - \bar{Y})}{\sqrt{\sum_{i=1}^n (X_i - \bar{X})^2} \sqrt{\sum_{i=1}^n (Y_i - \bar{Y})^2}}$$

where, X_i and Y_i are the individual data points of the two variables under comparison, here the MEI.v2 index and smoothed precipitation anomalies. \bar{X} and \bar{Y} are the means of the respective variables. n is the total number of data points. This coefficient allows us to understand better the strength and direction of the relationship between ENSO, represented by MEI.v2 index variation, and precipitation anomalies in the selected regions.

6.2.2 Results

The following Pearson correlation coefficients were computed for all six regions and showed a consistent pattern of negative values, refer to the Figure 6.2 and further being supported by the visual analysis plot, refer to the Figure 6.3. The negative values of the correlation coefficients mean that with the increased intensity of ENSO events, whether it be El Niño or La Niña—the precipitation anomalies for these regions generally go in the opposite direction. In North, Central, and South India, the negative values of the correlation coefficients agree with the known fact that El Niño acts in favour of drought or low monsoon rainfall over India and vice versa. La Niña favours active monsoon conditions. This inverse relation among ENSO phases and precipitation verifies that indeed the ENSO factor is strong in controlling the rainfall variability over India. The correlation results we observe between ENSO and India are consistent with the findings reported, Athira et al. (2023). They also found a weak correlation with central India among other parts of India. In Thailand, Malaysia and Thailand, the widely negative

Region	Correlation Coefficient
North India	0.396964
Central India	0.130382
South India	-0.221051
Thailand	-0.543576
Indonesia	-0.717252
Malaysia	-0.751909

Figure 6.4: ENSO-DJF Correlation Coefficient for Different Regions

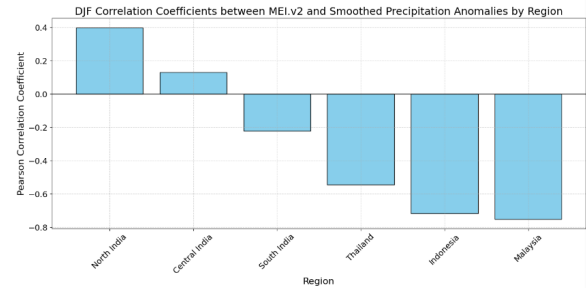


Figure 6.5: Correlation Coefficient MEI-DJF

correlations, particularly for Indonesia and Malaysia, mean that ENSO is a strong factor in these areas. During El Niño, which coincides with the positive MEI.v2 values, the region tends to be drier and often undergoes sharp decreases in rainfall. Its counterpart, La Niña, associated with the negative MEI.v2 values normally gives rise to wetter-than-usual conditions, showing an intense ENSO signal on the regional precipitation features. Our negative correlation of the MEI.v2 index with precipitation over Thailand, is in agreement with the outcome from the study by, Chueasa et al. (2024). This validate our results that La Niña indeed means higher precipitation in Thailand.

6.3 Seasonal Correlation Coefficient

As ENSO has sometimes a seasonally variable effect on precipitation, a seasonal comparison was done between MEI.v2 index and smoothed precipitation anomalies. The four seasons dealt were: DJF - December, January and February; MAM - March, April and May; JJA - June, July and August; and SON - September, October and November.

Let's take a look at the Figure 6.4 and Figure 6.5 for DJF seasonal correlation. The positive correlation indicates that El Niño tends to increase precipitation in this season in North India. This is a somewhat unusual result and might be affected by other factors such as the IOD. Central India has a weak positive correlation. Precipitation is foreseen to be less in El Niño according to the negative correlation derived for South India. Thailand, Indonesia, and Malaysia all have Strong Negative Correlations, particularly in Malaysia, and this would indicate that El Niño tends to result in drier conditions during this season.

Let's have a look at the Figure 6.6 and Figure 6.7, which is seasonal correlation coefficient for MAM. Southern India has moderate negative correlation thus indicates the decrease of the precipitation within the El Niño events. Thailand, Indonesia, and Malaysia have strong negative correlation that means significant ENSO impact within this season.

If you refer to the Figure 6.8 and Figure 6.9 for JJA seasonal correlation. We can see the strong negative correlation of North India reflects the well-documented impact of ENSO on the Indian monsoon. For South India, the strong negative correlation indicated El Niño tends to reduce rainfall during the monsoon season. Thailand, Indonesia, and Malaysia have Strong

Region	Correlation Coefficient
North India	0.095294
Central India	-0.071885
South India	-0.449359
Thailand	-0.758701
Indonesia	-0.512826
Malaysia	-0.755034

Figure 6.6: ENSO-MAM Correlation Coefficient for Different Regions

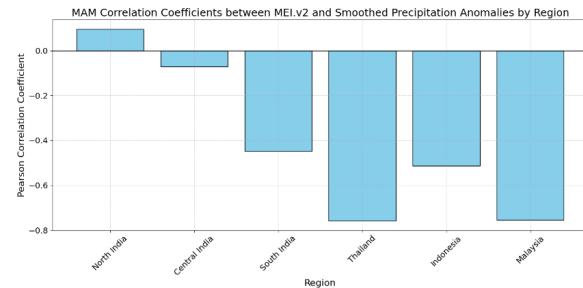


Figure 6.7: Correlation Coefficient MEI-MAM

Region	Correlation Coefficient
North India	-0.664237
Central India	-0.179025
South India	-0.550106
Thailand	-0.288110
Indonesia	-0.829486
Malaysia	-0.751713

Figure 6.8: ENSO-JJA Correlation Coefficient for Different Regions

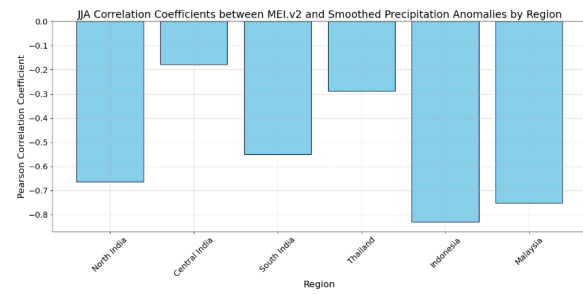


Figure 6.9: Correlation Coefficient MEI-JJA

negative correlations that highlighted ENSO's high magnitude of impact during this season.

In the Figure 6.10 and Figure 6.11 you could notice that while north India shows a high negative correlation, central India has shown a moderate negative correlation, and south India has shown a weak negative correlation. Strong negative correlations in Thailand, Indonesia, and Malaysia hint that ENSO continues to influence the precipitation pattern post-monsoon.

6.4 Significance Level Test

The consistent negative correlation across these regions suggests that ENSO indeed plays a critical role in modulating the precipitation patterns, with the typical response of El Niño suppressing rainfall and La Niña enhancing it. Having established the existence of such negative correlations, the subsequent task has been to check if these correlations are statistically significant. We will do this through a test of the significance level, which allows us to estimate the strength and reliability of the observed relationships between ENSO and regional precipitation patterns. In statistical analysis, we would often wish to test whether certain patterns are statistically significant in order to rule out that these results might be due to chance, and if the patterns are reliable. This can be done by the significance level test, where the following are key components: First, the Null hypothesis, which states no association between the two variables and hence any observed association is due to chance. Secondly, the Alternative hypothesis, which is opposite to the null and thus states that there exists a true association between variables, Scribbr (2020). The p-value is the probability that reflects the strength of evidence against the

Region	Correlation Coefficient
North India	-0.631246
Central India	-0.278172
South India	-0.222883
Thailand	-0.575363
Indonesia	-0.843472
Malaysia	-0.764057

Figure 6.10: ENSO-SON Correlation Coefficient for Different Regions

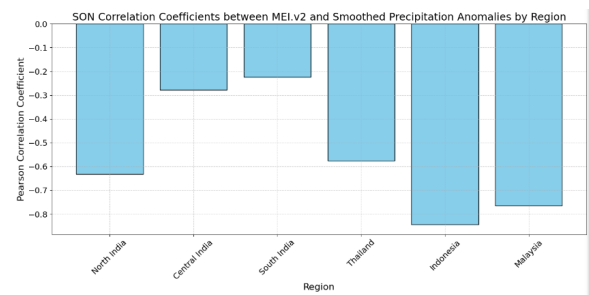


Figure 6.11: Correlation Coefficient MEI-SON

Region	p-value	Significant at 95%	Significant at 99%
North India	4.84×10^{-8}	True	True
Central India	3.90×10^{-3}	True	True
South India	5.02×10^{-10}	True	True
Thailand	1.00×10^{-16}	True	True
Indonesia	0.00×10^0	True	True
Malaysia	0.00×10^0	True	True

Table 6.1: Significance of p-values for Different Regions

null hypothesis. A small p-value is indicative of strong evidence against the null hypothesis. The significance level, denoted by α , can be considered to be 0.05 or 0.01 for 95% and 99%, respectively, it will dictate whether the p-value is sufficiently small to reject the null hypothesis. To test for significance in the Pearson correlation coefficient, denoted as r, we conduct a t-test. The t-statistic may be computed by the following formula:

$$t = \frac{r\sqrt{n-2}}{\sqrt{1-r^2}}$$

where, r = Pearson correlation coefficient. n = Number of paired observations i.e., Sample size the t-statistic follows a t-distribution with $n - 2$ degrees of freedom. The degrees of freedom are $n-2$ because the estimation of the correlation coefficient involves calculation of two means each of which consumes one degree of freedom. The Table 6.1 is the summary table of corresponding p-values for the correlation coefficient and the significance at 95% and 99% level of confidence. Where, in this case, the North India p-value of 0.000 confirms this correlation to be statistically significant at both 95% and 99% levels, which means the relationship is highly unlikely to be due to chance. Still, a p-value of 0.009 in Central India also intends that their statistical significance exists at both a 95% and 99% level. This reflects the small yet actual impact of MEI.v2 in the anomalies of precipitation within this region. Regions of South India, Thailand, Malaysia, and Indonesia show very significant p-values of 0.000. The results confirm that ENSO has a quite significant impact on precipitation anomalies within these regions. Statistical significance tests confirm that the negative correlations observed between MEI.v2 and smoothed precipitation anomalies are not the result of random chance but reflect a robust and real relationship.

6.5 Interpretation of Results

Analysis of the overall and seasonal correlations confirms the key role of ENSO in regional precipitation. The negative correlations across regions and seasons are consistent with the known climatological record, where El Niño tends to cause below-normal rainfall, and La Niña leads to above-normal rainfall in these regions. It is well expressed in India during the main stages of monsoon and post-monsoon seasons, JJA and SON, respectively where El Niño correlates with reduced rainfall. A positive correlation in North India is an exception during DJF and could be due to other climatic factors that may also nullify the impact of ENSO; for example, the IOD. In Southeast Asia, the influence of ENSO is strong throughout the year; in DJF, MAM, and SON, their negative correlations are very high. Such findings call for understanding seasonal variability in rainfall and adaptive strategies for mitigation to the impacts of ENSO on agriculture and water resources of these regions.

In other words, the ENSO climatic signal is being regarded, particularly, as the main driver of precipitation modes in analysed regions. The correlation between the MEI.v2 index and precipitation anomalies gives further insight into how specific regional climates are affected by events of ENSO, with an emphasis on strategy implementation for adaptation and mitigation impacts of climate variability.

Chapter 7

Correlation with climate signal: IOD

In the previous chapter, the correlation relationship was established for most regions between ENSO phases and precipitation patterns. However, ENSO is not the only climatic driver that controls these patterns. IOD (Indian Ocean Dipole), is another very important factor in climate variability but mainly in the Indian Ocean region and the surrounding areas. The following chapter now uses the results derived in Chapter 6 and seeks to investigate the relationship between the IOD and regional precipitation anomalies. In this regard, it attempts to complement what was learned from our ENSO analysis regarding the role of the IOD in determining the variability of precipitation.

7.1 Plotting Smoothed Precipitation Anomaly with IOD

To visually inspect the relationship between the IOD and regional precipitation we plotted the smoothed precipitation anomalies against the DMI time series for each of the regions. The regions will generally receive less rain during positive phases of the IOD, defined by the positive values of the DMI. We would expect increased precipitation with negative IOD phases. A number of patterns emerged from the Figure 7.1, in countries like Indonesia and Malaysia, the inverse relationship between the DMI-precipitation anomalies is clearly seen, in particular for strong positive phases of the IOD. This shows significant rainfall reductions within both countries. Thus, through this, it would also mean that these both countries are highly sensitive to variations in the IOD. For Thailand, the plot indicates that there is a fairly more distinct inverse relationship between the DMI and precipitation anomalies, in particular during those more extreme events of the IOD. This would, therefore, indicate that IOD is an influential factor in the precipitation of Thailand. In India, however, the relation between the DMI and precipitation anomalies was less distinct and more complicated. The plots were of a mixed pattern, where periods of positive DMI exist, although the relationship is not consistently strong throughout the time series. Specifically, over North and Central India, it would seem to indicate that though the IOD does influence the precipitation over India, there might be other climatic factors such as ENSO which could be more dominant in influencing the precipitation in these regions. The plot

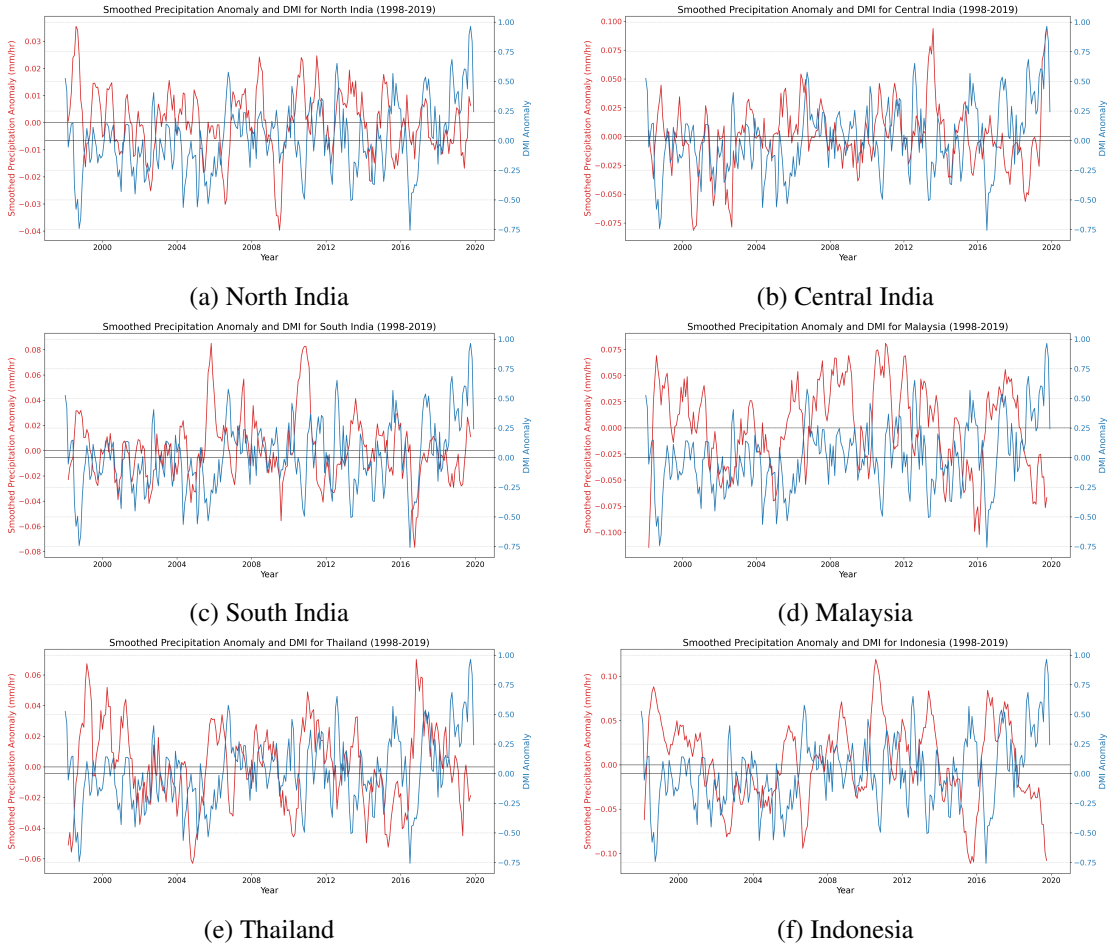


Figure 7.1: Smoothed precipitation anomaly with DMI plot for North India, Central India, South India, Malaysia, Thailand, and Indonesia.

for South India does indicate a weak inverse relationship of DMI with precipitation anomalies, it is much weaker than in Southeast Asia and thus suggests a more complex interplay of the climatic factors.

7.2 Correlation Coefficient between IOD and Precipitation Anomalies

The Pearson correlation coefficient was computed to quantify the relation between the IOD and regional precipitation anomalies. As a statistical measure, it gives an indication of the strength and direction in the linear relationship that exists between the DMI and the precipitation anomalies. As per the Figure 7.2 and Figure 7.3, It could be seen that most of the regions expressed predominantly negative correlations, which indicated positive phases of IOD. However, the strength of these correlations significantly varied between regions. In general, the DMI correlation coefficients show weaker relationships compared to ENSO. For example, there was

Region	Correlation Coefficient
North India	-0.084
Central India	-0.022
South India	-0.126
Thailand	-0.090
Indonesia	-0.386
Malaysia	-0.190

Figure 7.2: Pearson's Correlation Coefficient for DMI

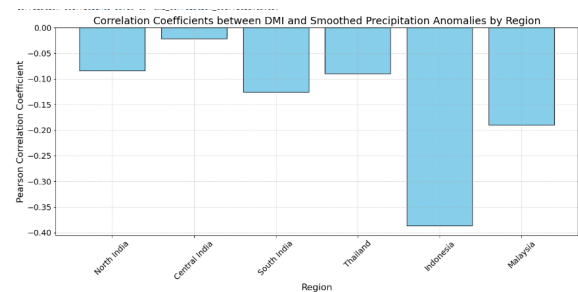


Figure 7.3: Correlation Coefficient DMI

Region	Correlation Coefficient
North India	0.035279
Central India	-0.118388
South India	-0.012354
Thailand	-0.134396
Indonesia	-0.285214
Malaysia	-0.103102

Figure 7.4: DMI-DJF Correlation Coefficient for Different Regions

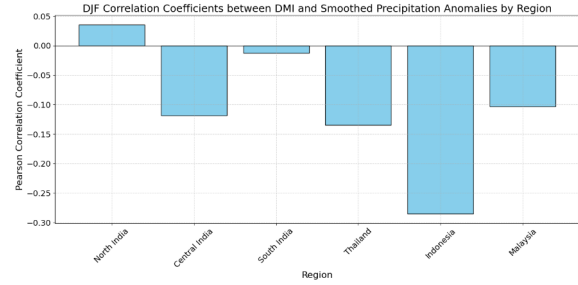


Figure 7.5: Correlation Coefficient DMI-DJF

a relatively strong negative correlation between Indonesia and Malaysia. This would be consistent with the known impacts of the IOD on rainfall in this area, in that there is a tendency for reduced precipitation, although the influence appears less robust compared to ENSO. On the contrary, North and Central India showed very low or near-zero correlations, insinuating the little influence IOD would have on its precipitation pattern. Generally speaking, the correlation for Thailand and South India suggests that the IOD does indeed have an impact on precipitation but to a somewhat weakened extent. These findings highlight the varying influence of the IOD across different regions, with Southeast Asia, particularly Indonesia, being more significantly affected.

7.3 Seasonal Correlation Coefficient

The IOD influence on precipitation could be seasonal in nature, so we conducted a seasonal analysis of the relationship between DMI and smoothed precipitation anomalies. We have considered the following four seasons: DJF-December-January-February, MAM-March-April-May, JJA-June-July-August, and SON-September-October-November.

The correlation coefficients for DJF, refer to the Figure 7.4 and Figure 7.5, suggest that the relationship between DMI and precipitation anomaly is weak over most regions. North India has a weak positive anomaly, which means a minimal effect from IOD; Central India and Malaysia have a weak negative correlation, which translates into some tendencies to have less rain in positive phases of IOD. South India remains almost neutral due to minimal influences from the IOD, while Indonesia and Thailand tend to have a pronounced negative correlation-where there

Region	Correlation Coefficient
North India	-0.013009
Central India	-0.211815
South India	-0.114648
Thailand	0.085979
Indonesia	0.165840
Malaysia	0.129016

Figure 7.6: DMI-MAM Correlation Coefficient for Different Regions

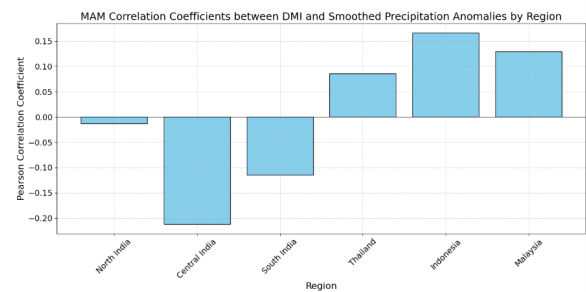


Figure 7.7: Correlation Coefficient DMI-MAM

Region	Correlation Coefficient
North India	0.032910
Central India	0.041423
South India	-0.116802
Thailand	0.030007
Indonesia	-0.293455
Malaysia	-0.121197

Figure 7.8: DMI-JJA Correlation Coefficient for Different Regions

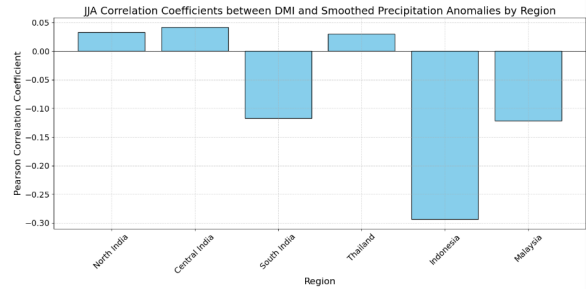


Figure 7.9: Correlation Coefficient DMI-JJA

is a greater tendency for drier-than-normal conditions in positive IOD phases. During the MAM season, refer to the Figure 7.6 and Figure 7.7, the relationship becomes more variable with the IOD. North India is very close to a zero correlation, hence little or no impact can be expected due to the IOD, while Central India presents a moderate negative correlation, which provides an indication of a possibility of below-normal rainfall during the positive phases of the IOD. In general, south India also shows a weak negative correlation, indicating a slight reduction in rainfall in positive IOD phases. Curiously enough, Indonesia and Malaysia show positive correlations during the season—that is, it seems that in these regions, positive IOD phases might lead to an increase in rainfall maybe due to interactions with other climatic factors. For the JJA season, refer to the Figure 7.8 and Figure 7.9, it is clear from correlations that the influence of IOD remains weak across India, with slight positive values over North, Central India, and Thailand thus indicating the negligible impact of IOD on monsoon rainfall. In South India, the negative correlation is appreciably weaker and contains the hint of reduced rainfall during positive phases. For Southeast Asia overall, Indonesia and Malaysia are the most dominating signals, both representing a stronger negative correlation and indicating that in this season, the positive phases are associated with large reduction in rainfall. In almost the whole domain, IOD has the strongest influence during the SON season for the region, refer to the Figure 7.10 and Figure 7.11. The North Indian region has a reasonably strong negative correlation, suggesting that positive IOD phases tend to reduce rainfall in this season. Central India remains near-neutral as in the preceding season with minimal IOD impact. However, South India, Thailand, Indonesia, and Malaysia show a stronger negative correlation, with Indonesia on the most significant re-

Region	Correlation Coefficient
North India	-0.314992
Central India	-0.005138
South India	-0.183871
Thailand	-0.337470
Indonesia	-0.708274
Malaysia	-0.586815

Figure 7.10: DMI-SON Correlation Coefficient for Different Regions

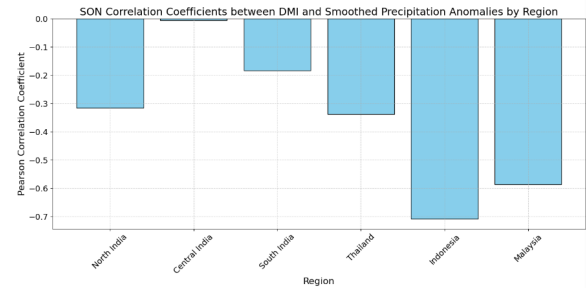


Figure 7.11: Correlation Coefficient DMI-SON

Region	p-value	Significant at 95%	Significant at 99%
North India	1.74×10^{-1}	False	False
Central India	7.26×10^{-1}	False	False
South India	4.13×10^{-2}	True	False
Thailand	1.45×10^{-1}	False	False
Indonesia	7.92×10^{-11}	True	True
Malaysia	1.95×10^{-3}	True	True

Table 7.1: Significance of p-values for Different Regions (DMI)

duction in rainfall during the positive IOD phases. This season highlights the major role of the IOD in the formation of regional precipitation, especially over Indonesia and Malaysia. From the seasonal analysis, there was a greater insight into how, through different seasons, the IOD affects the precipitation pattern differently and, therefore, calls for the consideration of seasonal variability in climate studies. The correlation coefficient analysis between ENSO, IOD, and precipitation patterns in Indonesia for seasonal correlations indicates that during JJA-SON, both ENSO and IOD have the highest impact on rainfall. This is in agreement with observations identified in the, As-Syakur et al. (2014), which further stipulates that indeed such seasons are those when rainfall is greatly responsive to the said climate phenomena.

7.4 Significance Level Test

We have performed a test of significance level for every region to rule out the possibility of obtaining these correlations between precipitation anomalies and DMI in these regions by random chance. It consisted of the calculation of p-values corresponding to the Pearson correlation coefficients and their comparison with the conventional levels of significance: at 95% probability with a p-value below 0.05 and at 99% probability with a p-value below 0.01. These tests will be important in confirming whether such correlations are statistically significant and not occur by mere chance. In the Table 7.1, Indonesia and Malaysia both are statistically significant negative correlation at 95% and at 99% significance, thus showing that IOD indeed has a strong impact on the precipitation patterns in these regions. South India exhibits a negative correlation significant at 95% probability, with the relative influence of the IOD being rather weak but still

significant. It gives statistically insignificant correlations for North India, Central India, and Thailand, which could represent that the IOD is not the major driver of precipitation anomalies in these regions; instead, other climatic factors are predominant. Also, nonsignificant results in some regions do not necessarily imply the absence of a relationship between the IOD and precipitation anomalies. It should be underlined that the no significance in some regions does not necessarily indicate an absence of a relationship between the IOD and precipitation anomalies; it could also be related to small effect sizes, noisy data, or even other climatic controls. Further studies with finer data may bring out the impact of the IOD on these regions.

7.5 Interpretation of Results

This analysis confirms that indeed IOD plays a modulating role with precipitation, especially over Southeast Asia, where its signal is most distinct in certain seasons-as shown in SON. Weaker correlations in the Indian regions signal that, though IOD might have an influence on precipitation, in general, it is less important than ENSO. Overall, the results suggest that the IOD is an important factor but part of a larger set of climatic drivers influencing regional precipitation. The IOD is a major driver of precipitation variability in regions such as Indonesia and Malaysia but particularly in its positive phase, which is associated with below-normal rainfall. For a region like India, the drivers of monsoon rainfall are likely to be dominated by other factors, including ENSO and possibly local monsoon dynamics. A non-significant result often indicates the need for further investigation. This could involve gathering more data, improving the precision of measurements, or considering additional variables that might influence the relationship. It is further very important to have such an understanding of this interaction of the mentioned climatic drivers with regard to developing effective water resources management, agriculture, and disaster preparedness strategies in these regions. The insights to be obtained in this chapter, together with insights from the analysis of ENSO in Chapter 6, will give a broader understanding of the climatic factors controlling precipitation variability in these regions.

Chapter 8

Introduction to EOF

We discussed regional precipitation anomalies concerning some of the significant climate drivers such as ENSO and IOD in Chapters 6 and 7. We viewed the correlation coefficients and time series for identifying the inverse relation that occurs between ENSO phases and precipitation patterns across regions like India, Thailand, Indonesia, and Malaysia. These analyses indeed had provided enough information on how these climatic phenomena influence regional precipitation. However, in as much as these methods are useful for establishing linear relationships, they might not be fully capable of representing the spatial variability and dominant modes of precipitation variability across those regions. In an attempt to overcome these shortcomings, we now discuss EOF analysis, a powerful technique for isolating the major spatial patterns of variation in a data set. The EOF analysis may also suggest those patterns that may not be directly apparent from the correlation or anomaly time series. It allows us to decompose the precipitation data into orthogonal modes and gives us a detailed view of how precipitation varies in space and time.

8.1 Concept and Methodology of EOF

EOF analysis can outline complicated spatial patterns and their relevant time evolution, this will be important in the understanding of regional climate dynamics, whereby one area might have high variability and modes dominating the precipitation patterns in these regions. We apply EOF analysis to raw precipitation data to indicate the main spatial patterns of variability, derive how such patterns change in time, quantify the amount of variance explained by each mode, thus yielding a clear picture of most influential patterns within the dataset. This shall complement our earlier findings and offer deeper insights into what could inform future climate modelling and prediction efforts, Bjornsson & Venegas (1997).

First, the raw precipitation data was loaded, a time index was created, and it was pivoted into a grid format where each row represents time, and each column represents a latitude-longitude pair. Data reshaped as a 3D NumPy array. This 3D array now serves as the basis for analysing the spatial and temporal precipitation patterns across regions. First, we loaded the 3D precipitation data for each region: time, latitude, and longitude. Three regions will be taken into

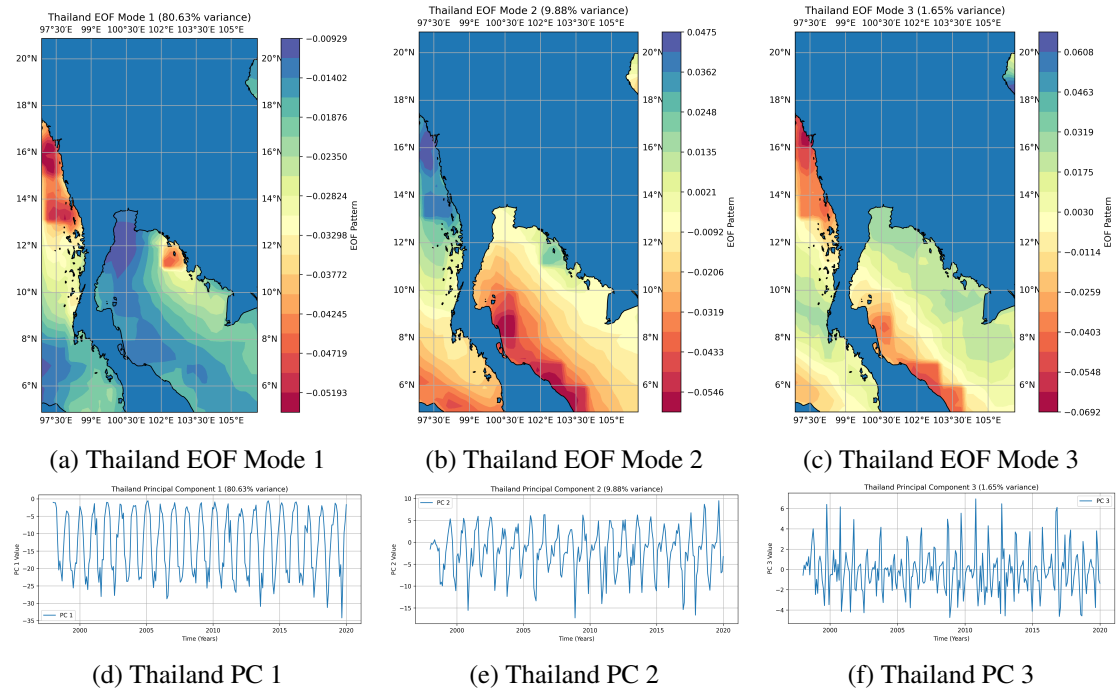


Figure 8.1: EOF Modes 1, 2, and 3, and PC 1, 2, and 3 for Thailand.

consideration in this analysis: South India, Thailand, and Indonesia. These three regions were previously identified by us as having the highest precipitation variability and most distinct patterns in a way that their comprehension is vital for the study of greater climate dynamics in the area. As we focus on these regions, it will be possible to go into great detail regarding the spatial and temporal variability that dominates these climates; such a focused approach will allow us to complement and build upon our earlier results. Then the 3D data was reshaped into a 2D array where each row represents a time point, and each column represents a grid point (latitude * longitude). We first calculated the covariance matrix of reshaped data to understand the variance structure of precipitation data. The covariance matrix was further subjected to eigen-decomposition, which gave rise to the eigenvalues and eigenvectors. Eigenvectors represent EOF modes, and the corresponding eigenvalues indicate variances explained by each mode. EOF modes were reshaped back into their spatial forms, thereby enabling us to visualize dominant precipitation patterns. The temporal development of these patterns is provided by the associated PCs.

8.2 EOF Analysis using raw precipitation data

In the case of Thailand refer to Figure 8.1, EOF Mode 1 explains 80.63% of the variance and reveals dramatic coastal variability, linked with the monsoon circulation. In concurrence with this mode of circulation, the first principal component is marked by pronounced seasonal peaks and troughs. EOF Mode 2, accounting for 9.88% of the variance, is confined to the southern

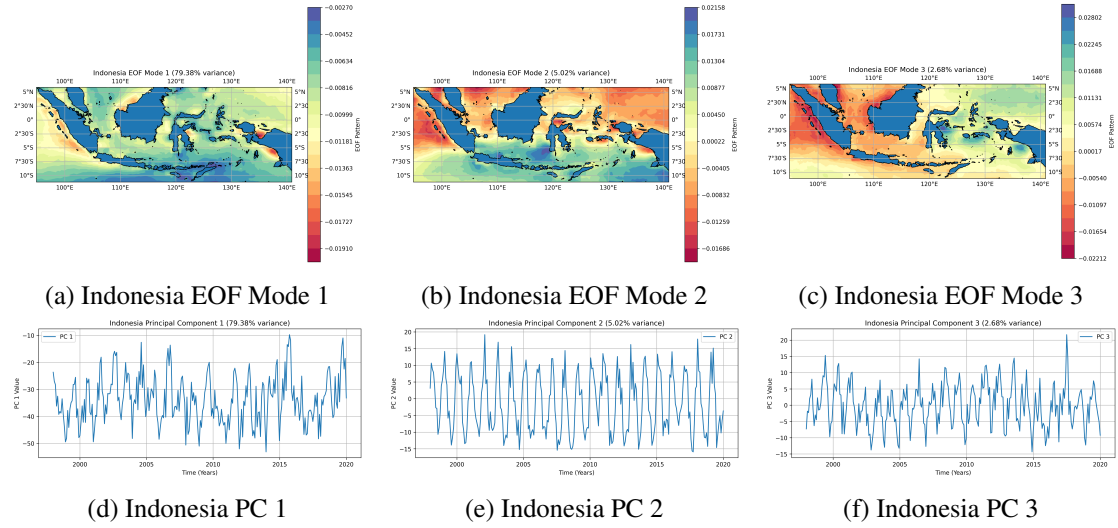


Figure 8.2: EOF Modes 1, 2, and 3, and PC 1, 2, and 3 for Indonesia.

areas and could be indicative of localized climatic or topographical influences. Shorter-term variability dominates in PC 2. EOF Mode 3 shows highly dispersed and less coherent variability across the region, while PC 3 with frequent localized fluctuations accounted for 1.65% of the variance. In the case of Indonesia, refer to the Figure 8.2, the first EOF mode explained 79.38% of the variance and PC 1 represent a dominant pattern that is most likely to be associated with the annual monsoonal cycle. The spatial pattern indicated a strong north-south gradient, possibly reflecting the seasonal shift in rainfall. The second mode is responsible for 5.02% of the variance and could implicate ENSO variability, considering it has a more regional effect, mainly toward the eastern parts of Indonesia. The third mode now shows even more localized and rather incoherent anomaly patterns with 2.68% of the variance, possibly reflecting shorter-period or secondary climatic influences.

The first order EOF mode for South India, refer to the Figure 8.3, it explains 70.16% of the variance, shows a strong north-south gradient in precipitation patterns, which reflects the dominant influence of seasonal monsoons across the region. This mode seemingly captures the annual cycle of the monsoonal rainfall. The second mode-one for 11.86% variance-similarly shared the same north-south signal but with a different spatial emphasis that may suggest interannual variability, probably related to phenomena like ENSO. The third mode is a more localized variability that could represent the intra-seasonal oscillation or shorter-term climatic events with a variance of 2.33%. These put together point toward the representation of both the annual cycles and wider climatic influences such as ENSO, making their presence felt within the precipitation dynamics of South India.

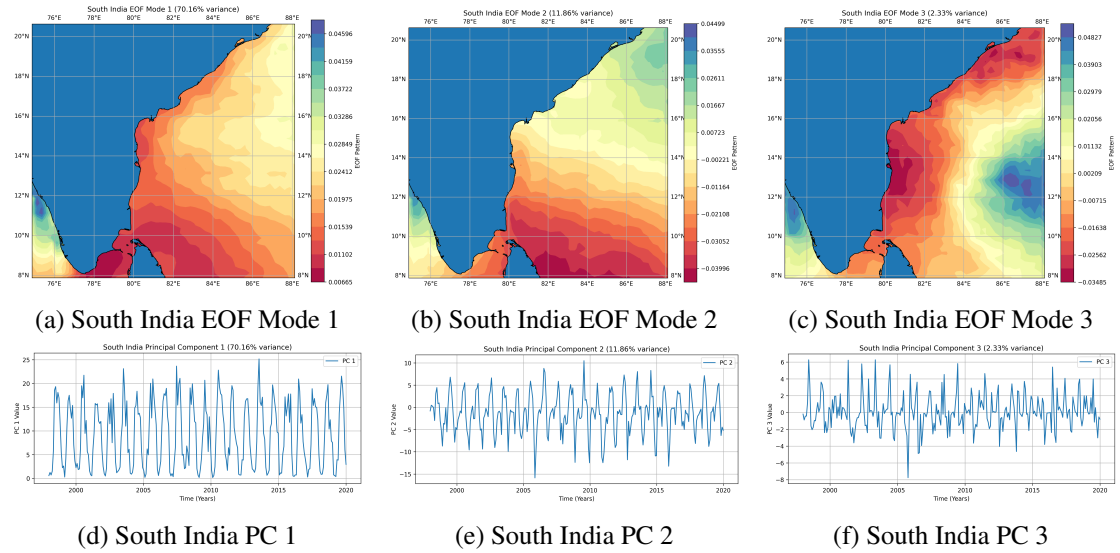


Figure 8.3: EOF Modes 1, 2, and 3, and PC 1, 2, and 3 for South India.

8.3 Summary

A characteristic common to the three modes is that over the land regions, variability is smaller than in coastal and oceanic regions. This can be the case because large landmasses stabilize precipitation as opposed to dynamic conditions over the ocean. Relatively lower variability over land may indicate that precipitation is more predictable and less prone to extreme changes compared to oceanic regions. In that respect, moving forward, the EOF analysis on precipitation anomalies rather than on raw data would be interesting to do; even more subtle patterns can then be identified when the seasonal cycle is removed and only the deviation from the mean state is considered. It would be a complementary study to the findings presented here and provide further insight into the drivers of the precipitation variability in this region. The results of EOF analysis in this study will be highly useful in many subsequent studies, especially in the developing seasonal forecasting models and for understanding the implication of climate variability on regional precipitation patterns.

Chapter 9

Conclusion

The findings from the paper further confirm the importance of the roles of ENSO and IOD in the control of rainfall over India and Southeast Asia. ENSO is inversely related to rainfall with a relatively high value, especially over Indonesia and Malaysia. The role of the IOD is limited, though very important in Southeast Asia. EOF analysis depicts that monsoonal cycles and large-scale climatic drivers are the main drivers of precipitation variability in these regions. It shows that for the understanding of climate impacts, both temporal and spatial patterns need to be considered and acts as a key input in the modeling of future climates, seasonal forecasting, and adaptation strategies in these climate-sensitive regions.

Bibliography

- As-Syakur, A. R. et al. (2014), ‘Observation of spatial patterns on the rainfall response to enso and iod over indonesia using trmm multisatellite precipitation analysis (tmpa)’, *International Journal of Climatology* **34**(15), 3825–3839.
- URL:** <https://doi.org/10.1002/joc.3939>
- Athira, K., Roxy, M. K., Dasgupta, P., Saranya, J., Singh, V. K. & Attada, R. (2023), ‘Regional and temporal variability of indian summer monsoon rainfall in relation to el niño southern oscillation’, *Scientific Reports* **13**(1).
- URL:** <https://doi.org/10.1038/s41598-023-38730-5>
- Bjornsson, H. & Venegas, S. A. (1997), ‘A manual for eof and svd analyses of climatic data’, <https://geog.mcgill.ca/gec3/wp-content/uploads/2009/03/Report-no.-1997-1.pdf>. Accessed: September 16, 2024.
- Chueasa, B., Humphries, U. & Waqas, M. (2024), ‘Influence of el niño southern oscillation on precipitation variability in northeast thailand’, *MethodsX* p. 102954.
- URL:** <https://doi.org/10.1016/j.mex.2024.102954>
- Climate Data Guide (2023), ‘Trmm: Tropical rainfall measuring mission | climate data guide’, <https://climatedataguide.ucar.edu/climate-data/trmm-tropical-rainfall-measuring-mission>. Accessed: September 16, 2024.
- Columbia Climate School (2019), ‘How climate change impacts our water’, <https://news.climate.columbia.edu/2019/09/23/climate-change-impacts-water/>. Accessed: September 16, 2024.
- Huffman, G. et al. (2015), ‘Trmm and other data precipitation data set documentation’, https://gpm.nasa.gov/sites/default/files/document_files/3B42_3B43_doc_V7.pdf. Accessed: September 16, 2024.
- Koad, P. & Jaroensutasinee, K. (2020), ‘Annual cycle of tropical and subtropical precipitation estimated from tmpa 3b42 dataset’, *Asia-Pacific Journal of Atmospheric Sciences* **57**(2), 235–260.
- URL:** <https://doi.org/10.1007/s13143-020-00192-4>

- NASA GES DISC (2024a), ‘Ges disc’, https://disc.gsfc.nasa.gov/datasets/TRMM_3B43_7/summary. Accessed: September 16, 2024.
- NASA GES DISC (2024b), ‘How to access ges disc data using wget and curl’, <https://disc.gsfc.nasa.gov/information/howto?title=How%20to%20Access%20GES%20DISC%20Data%20Using%20wget%20and%20curl>. Accessed: September 16, 2024.
- NASA Global Precipitation Measurement Mission (2024), ‘The tropical rainfall measuring mission (trmm)’, <https://gpm.nasa.gov/missions/trmm>. Accessed: September 16, 2024.
- NASA Jet Propulsion Laboratory (2024), ‘Indian ocean dipole (iod) index | vital signs – ocean surface topography from space’, <https://sealevel.jpl.nasa.gov/data/vital-signs/indian-ocean-dipole/>. Accessed: September 16, 2024.
- NOAA (2024), ‘What are el nino and la nina?’, <https://oceanservice.noaa.gov/facts/ninonina.html>. Accessed: September 16, 2024.
- NOAA Climate.gov (2020), ‘Meet enso’s neighbor, the indian ocean dipole’, <https://www.climate.gov/news-features/blogs/enso/meet-enso%E2%80%99s-neighbor-indian-ocean-dipole>. Accessed: September 16, 2024.
- OPENDAP HyrAx (2024), ‘Contents of /trmm3/trmm3b43.7/1998/’,. Accessed: September 16, 2024.
- Scheel, M. L. M., Rohrer, M., Huggel, C., Villar, D. S., Silvestre, E. & Huffman, G. J. (2010), ‘Evaluation of trmm multi-satellite precipitation analysis (tmpa) performance in the central andes region and its dependency on spatial and temporal resolution’, *Hydrology and Earth System Sciences Discussions* .
- URL:** <https://doi.org/10.5194/hessd-7-8545-2010>
- Scribbr (2020), ‘An introduction to t tests | definitions, formula and examples’, <https://www.scribbr.com/statistics/t-test/>. Accessed: September 16, 2024.
- Scribbr (2022), ‘Pearson correlation coefficient (r) | guide & examples’, <https://www.scribbr.com/statistics/pearson-correlation-coefficient/>. Accessed: August 8, 2024.
- Singh, T. P., Kumbhar, V., Das, S., Deshpande, M. M. & Dhoka, K. (2019), ‘Comparison of trmm multi-satellite precipitation analysis (tmpa) estimation with ground-based precipitation data over maharashtra, india’, *Environment Development and Sustainability* 22(6), 5539–5552.
- URL:** <https://doi.org/10.1007/s10668-019-00437-x>
- Stallard, M. & E. (2024), ‘What are el niño and la niña, and how do they change the weather?’, <https://www.bbc.co.uk/news/science-environment-64192508>. Accessed: September 16, 2024.

- Stseo (2020), ‘Changing rainfall patterns & its effect on agriculture | sourcetrace systems’, <https://sourcetrace.com/blog/changing-rainfall-patterns-effect-agriculture#:~:text=An%20important%20aspect%20to%20be,germination%20and%20fruit%20development%20stage>. Accessed: September 16, 2024.
- Tableau (n.d.), ‘Time series analysis: Definition, types, techniques, and when it’s used’, <https://www.tableau.com/learn/articles/time-series-analysis>. Accessed: September 16, 2024.
- Team, P. (2024), ‘Multivariate enso index version 2 (mei.v2)’, <https://psl.noaa.gov/enso/mei/>. Accessed: September 16, 2024.
- World Bank Climate Change Knowledge Portal (2024a), ‘Climate data - historical: India’, <https://climateknowledgeportal.worldbank.org/country/india/climate-data-h#:~:text=India%20has%20a%20tropical%20climate,hottest%20months%20of%20the%20year>. Accessed: August 10, 2024.
- World Bank Climate Change Knowledge Portal (2024b), ‘Climate data - historical: Indonesia’, <https://climateknowledgeportal.worldbank.org/country/indonesia/climate-d#:~:text=Indonesia%20has%20a%20tropical%20climate,hottest%20months%20of%20the%20year>. Accessed: August 10, 2024.
- World Bank Climate Change Knowledge Portal (2024c), ‘Climate data - historical: Malaysia’, <https://climateknowledgeportal.worldbank.org/country/malaysia/climate-d#:~:text=Malaysia%20has%20a%20tropical%20climate,hottest%20months%20of%20the%20year>. Accessed: August 10, 2024.
- World Bank Climate Change Knowledge Portal (2024d), ‘Climate data - historical: Thailand’, <https://climateknowledgeportal.worldbank.org/country/thailand/climate-d#:~:text=Thailand%20enjoys%20a%20tropical%20climate,country%2C%20especially%20the%20mountainous%20regions>. Accessed: August 10, 2024.